

ZnTe/GaAs(001): Growth mode and strain evolution during the early stages of molecular-beam-epitaxy heteroepitaxial growth

V. H. Etgens,* M. Sauvage-Simkin,[†] R. Pinchaux,[‡] J. Massies,[§] N. Jedrecy,[†]
A. Waldhauer,** S. Tatarenko,^{††} and P. H. Jouneau,^{§§}

*Laboratoire pour l'Utilisation du Rayonnement Electromagnétique, CNRS, Commissariat à l'Énergie Atomique,
Ministère de l'Éducation Nationale et de la Culture, Bâtiment 209d,
Centre Universitaire, 91405 Orsay CEDEX, France*

(Received 3 August 1992; revised manuscript received 10 November 1992)

The initial stages of molecular-beam-epitaxy heteroepitaxial growth of ZnTe on GaAs(001) substrates are studied by *in situ* grazing incidence x-ray diffraction performed under ultrahigh vacuum. Pseudomorphic fully strained layers are observed for deposits up to 4 molecular layers (ML), whereas plastic relaxation starts after a critical thickness of about 5 ML together with the onset of a three-dimensional growth mode. Evidence for a normal strain gradient is obtained in partially relaxed layers. The results are confirmed by *ex situ* high-resolution transmission electron microscopy.

I. INTRODUCTION

The growth of crystalline thin films has been recognized as an important field of research for which several techniques have been implemented. The ultimate goal is to tailor and combine different materials in order to obtain the desired electronic properties. Epitaxial films having different lattice parameters can now be grown coherently on a single substrate. One can then match previously selected electronic properties of the film with the advantages presented by the substrate. However, the conditions which allow the formation of a coherent epitaxial film on a different monocrystalline substrate are still poorly understood.

The present work is concerned with the epitaxial growth of ZnTe, a II-VI semiconductor compound, on GaAs(001) substrates by molecular-beam epitaxy (MBE). This III-V material is preferred to ZnTe substrates due to its better crystalline quality and to the availability of large single crystals, a critical feature for the industrial production of devices.

ZnTe and GaAs both crystallize in the zinc-blende structure with lattice parameters equal to 6.10 and 5.65 Å, respectively, at room temperature, giving a lattice mismatch of 7.9%. The interest of ZnTe growth on GaAs(001) lies primarily in the production of a buffer layer for the subsequent growth of CdTe/Cd_{1-x}Hg_xTe (Ref. 1) superlattices and heterostructures in the (100) orientation on GaAs substrates. The lattice parameter, intermediate between those of GaAs and CdTe (6.48 Å), is well suited for this purpose. A further application is found in the elaboration of ZnTe/CdTe (Ref. 2) or ZnTe/ZnSe (Ref. 3) strained superlattices.

When an epilayer is grown on a substrate having a slightly different lattice parameter two cases are expected: If the surface free energy of the epilayer is higher than that of the substrate, three-dimensional (3D) growth occurs as predicted by the theory of wetting phenomenon (Volmer-Weber growth mode). Otherwise, if the surface free energy of the epilayer is lower than that of the sub-

strate and also the lattice mismatch is low enough to be elastically accommodated a two-dimensional growth can occur. The epilayer is then strained to match the substrate parameter in the interface plane and, as a consequence, suffers an opposite strain in the out-of-plane direction. For cubic structures with a (001) interface, this deformation is tetragonal. The energy stored in the layer is proportional to its thickness in the elastic regime and this process is thus limited: beyond a certain thickness, plastic relaxation of the layer becomes energetically favorable and dislocations are generated in the film. The defects then produced bring the film to a relaxed state with the misfit being accommodated by the dislocation network. The critical thickness can be defined as that for which the first misfit dislocation is formed. Even though many theories have been proposed to describe the strain distribution in the layer and to predict the critical thickness value, they are still quite sample specific which explains why so many controversies can be found in the literature. Once the critical thickness is reached, the defects present in the layer frequently promote an islanding of the film. This growth mode, characterized by a 2D-3D transition around the critical thickness, is called Stranski-Krastanov mode and has been observed for strained systems like CdTe/ZnTe,⁴ Ge/Si(001),⁵ and Ga_xIn_{1-x}As/GaAs.⁶ Nevertheless, it does not seem clear whether the defects (misfit dislocations) are responsible for the islanding or if the islanding happens first, the defect generation then being favored by the increased roughness, at least for some systems.^{5,7}

Recently more attention has been paid to the first few angstroms near the interface and to the state of the substrate surface which can determine the equality of the whole film. For the growth of CdTe on GaAs,⁸ for example, it was shown that the selection of a precursor surface, with a given bonding configuration, determines the film growth direction ([100] or [111]). The exact knowledge of the mechanism underlying the growth process necessarily requires a description of atomic configuration at the interface and consequently of the

precursor states of the growth.⁹

Grazing incidence x-ray diffraction (GIXD) performed in ultrahigh vacuum (UHV),¹⁰ on samples prepared *in situ* by molecular beam epitaxy, has been used to measure the in-plane strain in the very first stages of ZnTe/GaAs(001) heteroepitaxial growth. The x-ray measurements were performed at the LURE (Orsay-FR) synchrotron radiation facility using the unique coupling of a UHV compatible 4-circle diffractometer with a sample preparation chamber providing both II-VI and III-V MBE growth capabilities. *Ex situ* high-resolution transmission electron microscopy (HRTEM) was performed for some samples in order to characterize the defects present in the film as well as for an accurate thickness calibration.

II. EXPERIMENT

GaAs(001) wafers, cut better than 0.05° of the nominal orientation were introduced in the UHV just after degreasing. They were outgassed at 350°C and then transferred to the main MBE chamber. Deoxidation took place at 600°C under an As pressure of 2×10^{-6} mbar. A diffuse 2×4 reflection high-energy electron diffraction (RHEED) pattern was then observed and a few hundred nanometers thick GaAs buffer layer was grown using normal GaAs(001) MBE conditions: substrate temperature of 580°C , growth rate of 0.5 monolayer (ML)/s. The buffer layer improved the surface smoothness, which was confirmed by the sharp 2×4 RHEED pattern then observed. When cooled down to 400°C under the arsenic flux, the 2×4 reconstructed phase transformed into a $c(4 \times 4)$ reconstruction characterized by 0.75 ML of dimerized As atoms chemisorbed on a bulk like As top layer.¹¹ At this level the shutter of the As effusion cell was closed and the sample temperature kept at 250°C . After a wait of a few hours for the pressure to recover to the 10^{10} mbar range, the heteroepitaxial growth of ZnTe was performed on the $c(4 \times 4)$ GaAs(001) surface. The ZnTe was provided by an extra effusion cell with a boron nitride crucible appended to the main chamber and surrounded by two liquid-nitrogen-cooled shrouds. This arrangement ensured a highly collimated flux thus reducing the contamination in the main chamber where the base pressure during evaporation remained below 10^{-9} mbar. The substrate temperature was kept at 320°C during the deposition and a ZnTe growth rate of about 0.2 ML/s was used. Successive exposures were performed on the same substrate with the sample alternately transferred from the MBE chamber to the UHV diffractometer stage under UHV, without exposure to atmosphere. When GIXD data collection was completed, some samples were studied by HRTEM in cross-section mode, providing at the same time an overview of the defects present in the film and an *a posteriori* thickness calibration. GIXD data were collected at the critical incidence angle for GaAs: $\alpha_c = 0.28^\circ$ with $\lambda = \lambda K_{\text{Ni}} = 1.488 \text{ \AA}$ using the x rays from a DCI non-focused bending magnet beam line, monochromatized by a Si(111) channel cut crystal. The grazing incidence angle is thus defined to better than $\alpha_c/10$ whereas the slit in

front of the detector integrates the grazing exit angle over about 1° . To avoid strain induced by the indium mounting, the sample was kept at 200°C , above the indium melting point, during data collection.

The GIXD results presented here are only concerned with the ZnTe growth on a $c(4 \times 4)$ GaAs(001) substrate using a stoichiometric flux of ZnTe. A similar ZnTe epitaxial growth was also observed by RHEED using a reconstructed $\sqrt{3} \times \sqrt{3}$ Te-GaAs(001) (Ref. 12) precursor surface but no GIXD measurements were performed.

III. RESULTS AND DISCUSSION

Preliminary RHEED experiments have shown a two-dimensional growth for the first few monolayers after which islands start to develop which confirmed the results obtained by Cibert *et al.*⁴ with the same technique. In order to follow precisely the beginning of growth, GaAs $c(4 \times 4)$ fractional order reflections were monitored after ZnTe deposition by GIXD. The $c(4 \times 4)$ surface characteristic peaks disappeared as soon as one monolayer equivalent thickness of ZnTe was deposited. There was still the possibility that the Te atoms alone could stick to the As rich surface leading to 6×1 or 2×1 (Ref. 12) Te-GaAs reconstructions which would equally destroy the $c(4 \times 4)$ GaAs reconstruction. The search for these specific superstructures was not successful, indicating a homogeneous 2D ZnTe growth at this level.

To characterize the strain at the interface, the in-plane relative lattice parameter difference between the epilayer

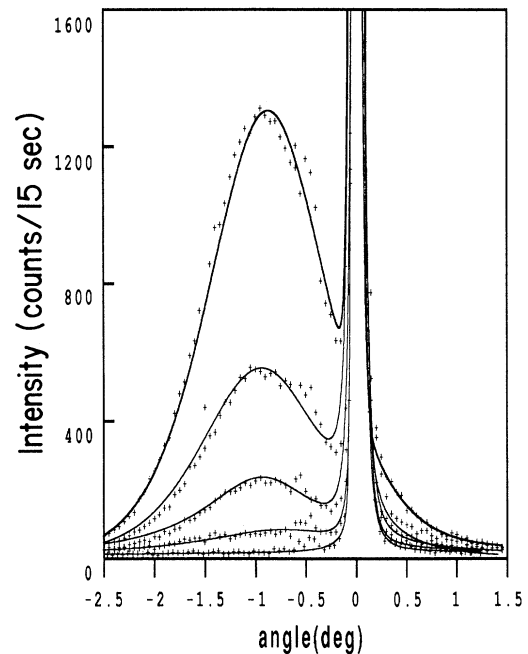


FIG. 1. θ - 2θ scans of the (200) reflection from ZnTe/GaAs (001) for heterostructures of increasing thicknesses (4, 6, 7, 9, and 15 ML from bottom to top curve). Profiles are aligned on the substrate Bragg peak.

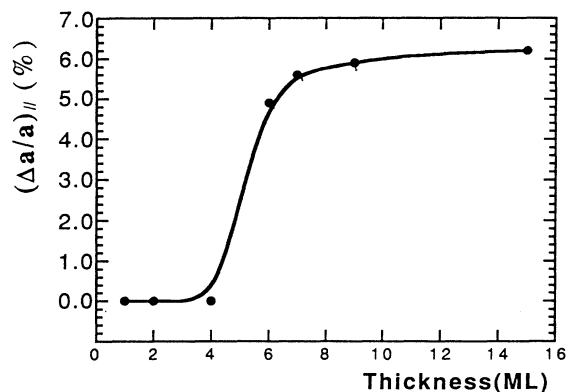


FIG. 2. Variation of $(\Delta a/a)_{\parallel}$ with the film thickness.

and substrate, $(\Delta a/a)_{\parallel}$, was measured through the Bragg angle peak shift $\Delta\theta$ for the (200) reflection, using the expression

$$(\Delta a/a)_{\parallel} = -\Delta\theta \cot\theta .$$

This reflection was chosen since it is very weak in GaAs and would improve the signal ratio between the epilayer and the substrate. The elastic strain in the epi-

layer parallel to the interface is thus

$$\epsilon = (\Delta a/a)_{\parallel} - f ,$$

where f is the relative bulk lattice parameter difference.

A series of radial scans (θ - 2θ) in reciprocal space, recorded for successive depositions, is displayed in Fig. 1. The presence of a ZnTe epilayer is undetectable for thicknesses up to 4 ML, which indicates a purely elastic accommodation of the misfit, with a maximum parallel compressive strain e of 7.9%. After 6-ML deposition, a bump satellite appears on the low angle side of the substrate Bragg peak corresponding to partially relaxed ZnTe [$(\Delta a/a)_{\parallel} = 4.9\%$]. As expected, the amount of plastic relaxation increases with the thickness of the epilayer. A plot of the relaxation $(\Delta a/a)_{\parallel}$ as a function of the film thickness is presented in Fig. 2. It illustrates the abrupt transition from elastic to plastic accommodation of the misfit strain between 4 and 6 ML. This transition is also associated with the onset of island growth on the film as shown by HRTEM pictures (Figs. 3-5). Figure 3 shows a rather homogeneous film indicating that islanding takes place mostly after the beginning of plastic relaxation.

Several comments should be made concerning these data. First, the small integrated intensity from the par-

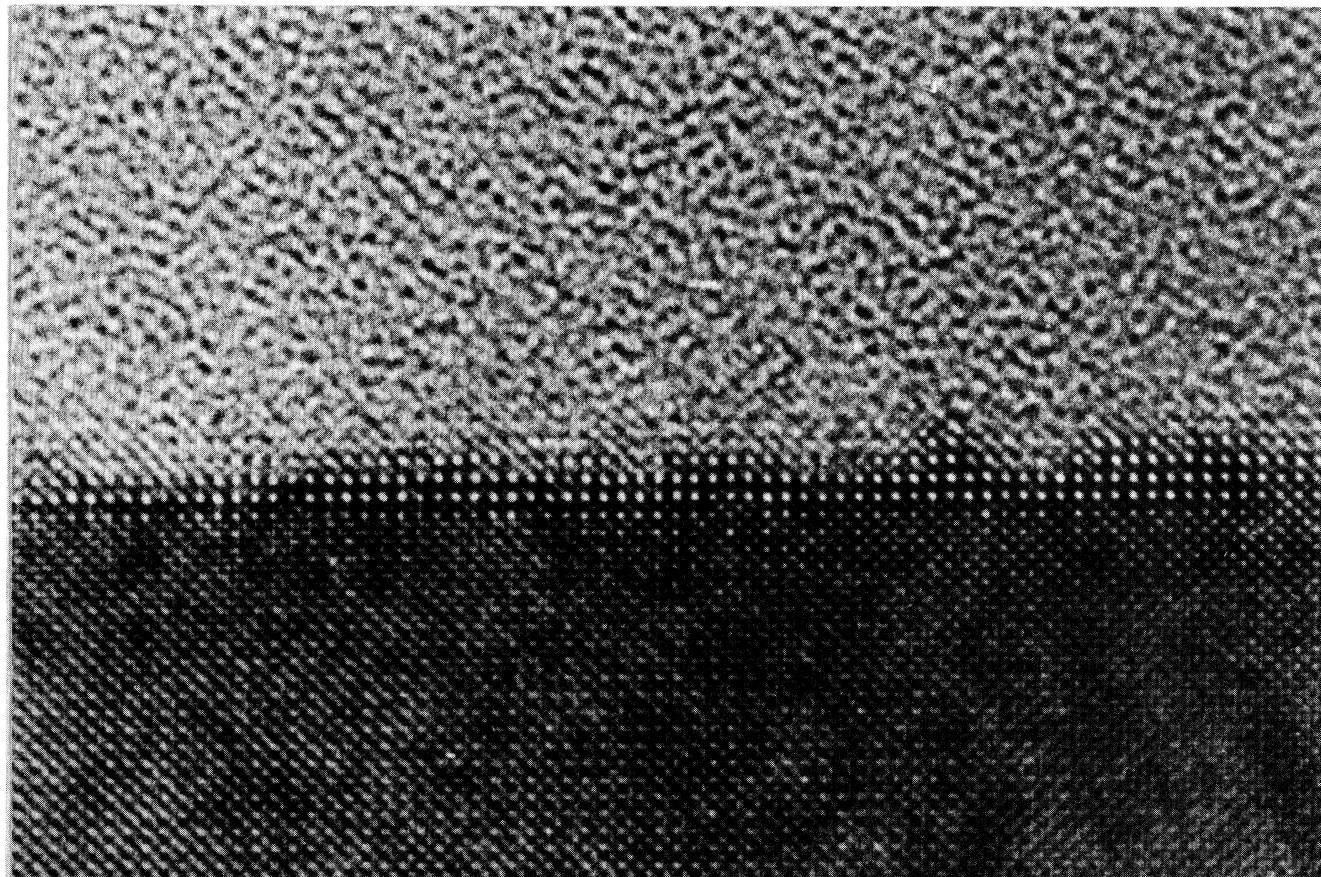


FIG. 3. HRTEM [100] cross section of 2-ML strained ZnTe on GaAs(001) (400 keV).

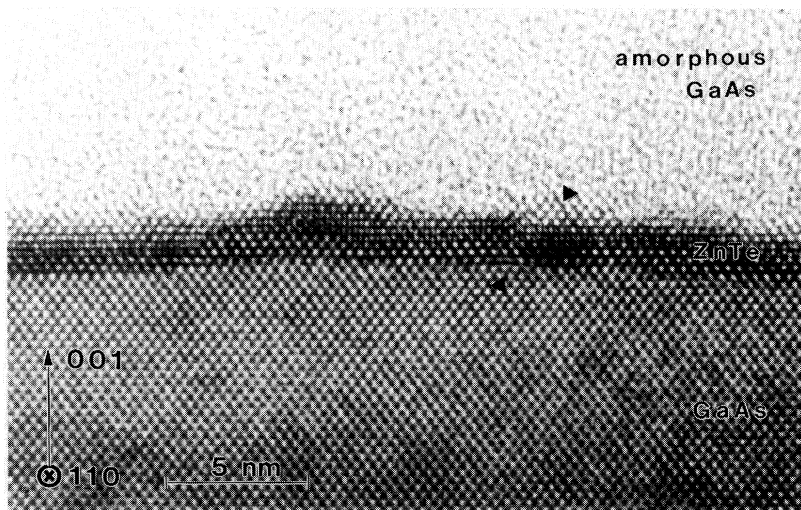


FIG. 4. HRTEM [110] cross section of 5-ML strained ZnTe on GaAs(001) (400 keV), the arrow points to an interface defect in a locally thicker area.

tially relaxed 6-ML film is possibly due to lateral thickness inhomogeneities in the film implying that the critical value is exceeded only for a fraction of the whole irradiated thin layer. This hypothesis is confirmed by HRTEM images (Fig. 4) where, for a nominal 5-ML-thick sample, both dislocation free (4 ML local thickness) and partially relaxed areas (7 ML locally) are detectable: a dislocation

located close to the interface is denoted by the arrows in Fig. 4. From these data, the critical thickness for the system is then equally inferred at 5 ± 1 ML (15 \AA). This value is identical to the critical thickness determined for CdTe/ZnTe (lattice mismatch of 6%) by means of RHEED oscillations.⁴ Second, the apparent saturation value of plastic relaxation (about 6.2%) shown in Fig. 2 is

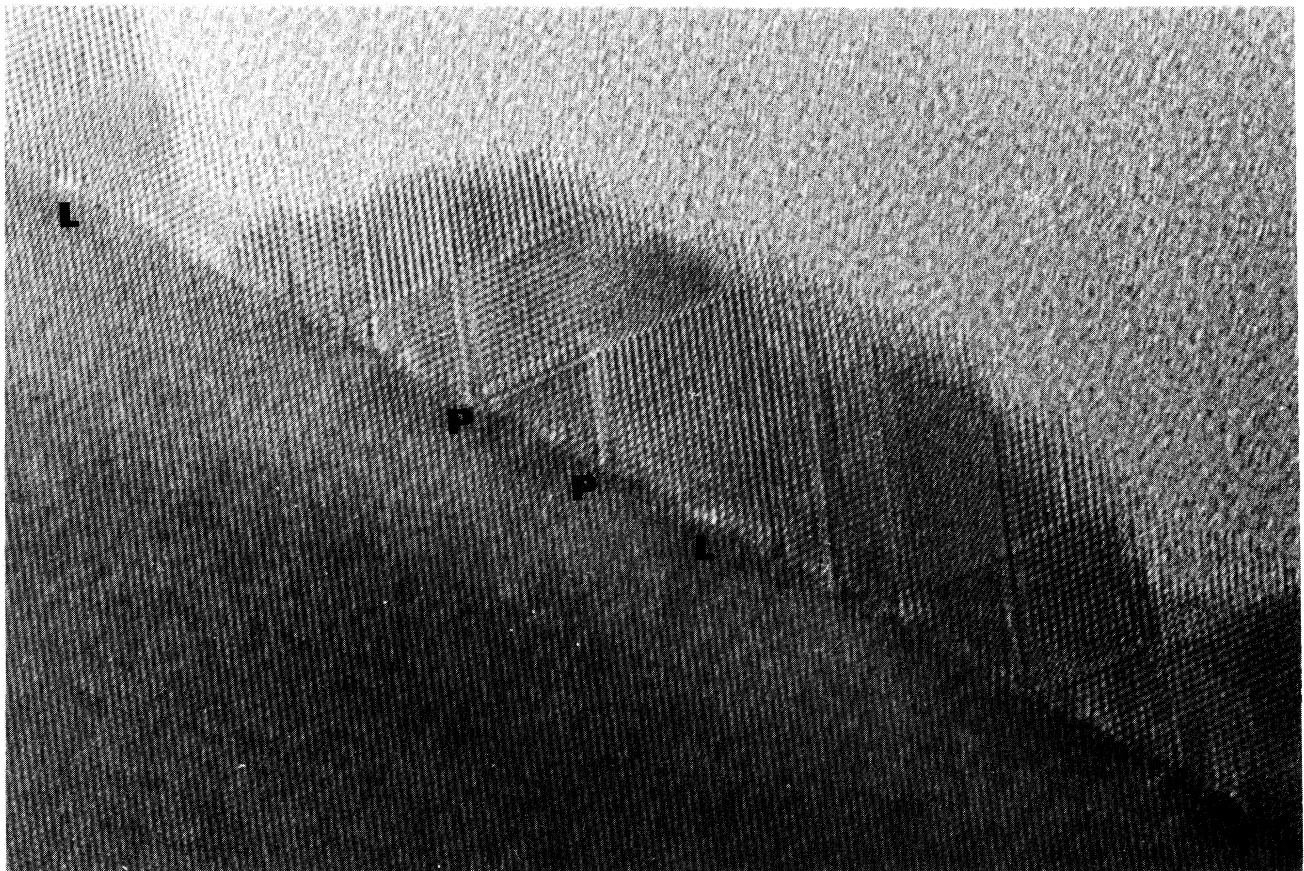


FIG. 5. HRTEM [110] cross section of 35 ML of ZnTe on GaAs(001) (400 keV). Interfaces defects such as Lomer (*L*) and partial (*P*) dislocations are imaged.

much smaller than the bulk value (7.9%). In order to clarify this point, the strain in the epilayer was determined under conditions of different surface sensitivity. This is made possible by tuning the penetration depth for x-rays with the grazing incidence angle. An incident angle equal to the critical value for total reflection (α_c) gives for ZnTe at $\lambda=1.488$ Å a penetration depth (defined as the $1/e$ attenuation of the transmitted intensity¹³) equal to 103 Å, as a consequence, for a 50-Å-thick epilayer, the diffraction signal carries an information averaged over the whole layer. The reduction of the incident angle to $0.3\alpha_c$, for example, reduces the penetration depth to 23 Å and the diffraction signal is mostly sensitive to the few layers near the surface. It is then possible to investigate the strain gradient in the epilayer. Figure 6 presents the angular scans performed at two different incidence angles for a 15-ML (45-Å) thick epilayer. The measures at $0.3\alpha_c$ yield a relaxation value of 7.0% which is closer to 7.9%, corresponding to the bulk ZnTe/GaAs lattice parameter mismatch, compared to the average value of 6.2%. The gradient thus detected showed a stronger relaxation for the top layers probably allowed by an elastic deformation through the island free surfaces. In addition, the correlation length of the epitaxial layer,¹⁴ is seen to slightly increase from an average value of 119 Å to a surface value of 130 Å. A similar effect was observed in the case of GaAs/Si(001) (Ref. 15) and Ge/Si(001).⁶

We did not observe the two distinct zones of relaxation as described by Patrat *et al.*¹⁶ but more likely a homogeneous distribution of the misfit gradient along the perpendicular to the interface direction is found. The sharp peak visible in between the GaAs and ZnTe maxima (Fig. 1) is a parasitic peak from the GaAs substrate which is there even prior to ZnTe deposition.

The stepwise deposition of ZnTe on GaAs is not necessarily identical to an uninterrupted growth: a layer degradation and/or kinetic factors could disturb the growth: in some cases, the separation between two successive depositions was as large as several hours. To address this question, two samples were directly prepared in the same conditions, as far as possible, with thicknesses

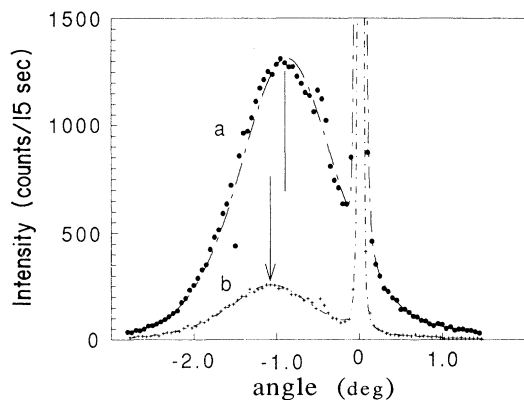


FIG. 6. Radial scans of the 15-ML ZnTe/GaAs at different inside angles. (curve a) $\alpha = \alpha_c$; (curve b) $\alpha = 0.3\alpha_c$.

TABLE I. Numerical value of the in-plane lattice parameter mismatch for successive deposited thicknesses.

Equivalent thickness (ML)	Thickness (Å)	$\Delta a/a_{\parallel}$ (%)
4	12.20	...
6	18.30	4.9
7	21.35	5.6
9	27.45	5.9
15	45.75	6.2

of 4 and 6 ML, respectively. For the 4-ML sample no relaxation was detected. In the case of the 6-ML-thick sample, a relaxation with an average misfit equal to 6.5% was observed. These measurements are in fair agreement with the previous ones, obtained with successive depositions (Table I), if one takes into account the uncertainty in the deposited thickness.

Taking advantage of a heater located on the diffractometer stage, we investigated the effect of annealing on the strain in the layer. A 10-ML-thick ZnTe/GaAs was prepared and successive angular scans were recorded at different temperatures after stabilization of the thermocouple display. The measured $(\Delta a/a)_{\parallel}$ increased from 5.8% (partially relaxed layer) at room temperature, to 7.9% (fully relaxed layer) at 300°C (Fig. 7). The observed intensity decrease of the ZnTe peak at 300°C is probably associated with the degradation of the film heated in UHV. Two main effects can be responsible for the increase in strain relaxation with temperature: (a) defect generation is favored by the extra energy available in the system; (b) the mobility of the dislocations is enhanced.

HRTEM was also used to identify the type of defects involved in the strain relaxation process. Figure 5 presents a HRTEM picture of a 100-Å ZnTe epilayer deposited on a GaAs substrate. Two different defects can be identified at the interface: (i) pure edge "Lomer" sessile dislocations (L) which are most efficient to relax the in plane strain since their Burgers vector is parallel to the

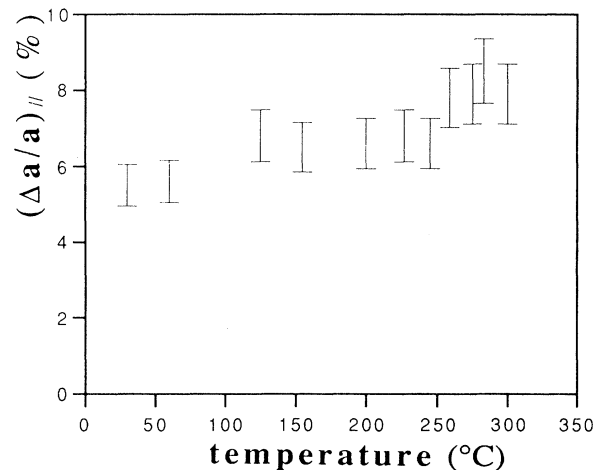


FIG. 7. Evolution of the strain relaxation in a 10-ML-thick ZnTe/GaAs(001) heterostructure with temperature.

interface; (ii) partial dislocations (P) bounding intrinsic and extrinsic stacking faults ending at the interface.

The variety of the defects precludes any periodic array which could lead to an interface superstructure as has been observed in other heteroepitaxial systems [GaSb/GaAs(001) (Refs. 17 and 18) or CdTe(111)/GaAs(001) (Ref. 19)].

IV. CONCLUSION

Grazing incidence x-ray diffraction has been applied to study the strain accommodation in the first stages of the epitaxial growth of ZnTe on GaAs(001) prepared in situ by molecular beam epitaxy. Accurate measurements of the in-plane mismatch, provided by this technique, have enabled us to confirm a fully strained epilayer growth up to 5 ± 1 ML. Above this critical thickness value, plastic

relaxation is detected in the x-ray data and confirmed by *ex situ* HRTEM experiments. HRTEM allows one to correlate the trespassing of the critical thickness for plastic relation with the transition between a layer-by-layer and an island growth mode, already observed by RHEED. The ability of x-ray diffraction to probe a thin heterostructure from the top surface to buried interfaces makes it an invaluable tool to investigate growth mechanisms in a quantitative and nondestructive manner.

ACKNOWLEDGMENTS

One of us (V.H.E.) acknowledges the financial support of the Brazilian CAPES. The Laboratoire de Minéralogie-Cristallographie and the Laboratoire de Spectrométrie Physique are Unité associée au Centre National de la Recherche Scientifique.

*Present address: European Synchrotron Radiation Facility, BP 220, 38043 Grenoble CEDEX, France.

†Also at Laboratoire de Minéralogie and Cristallographie, 4 place Jussieu, 75252 Paris CEDEX, France.

‡Also at Université Pierre et Marie Curie, 75230 Paris CEDEX, France.

§Also at Laboratoire de Physique du Solide et Énergie Solaire, rue B. Gregory, 06560 Valbonne, France.

**Also at DRECAM, Commissariat à l'Énergie Atomique, Gif-sur-Yvette, France.

‡Also at Laboratoire de Spectrométrie Physique, Université Joseph Fourier, Grenoble, France.

§§Also at Département de Recherche Fondamentale, Centre d'Études Nucléaires de Grenoble, Boîte Postale 85X, 38041 Grenoble CEDEX, France.

¹G. Monfroy, S. Sivananthan, X. Chu, P. Fourie, R. D. Knox, and J. L. Staudenmann, *Appl. Phys. Lett.* **49**, 152 (1986).

²B. K. Wagner, J. D. Oakes, and C. J. Summers, *J. Cryst. Growth* **86**, 296 (1988).

³H. Lou, N. Samarth, F. C. Zhang, A. Pareek, M. Dobrowolska, and J. K. Furdyna, *Appl. Phys. Lett.* **58**, 1783 (1991).

⁴J. Cibert, R. André, C. Deshayes, G. Feuillet, P. H. Jouneau, Le Si Dang, R. Mallard, A. Nahmani, K. Seminadayar, and S. Tatarenko, *Superlattices Microstruct.* **9**, 271 (1991).

⁵A. A. Williams, J. M. C. Thornton, J. E. McDonald, R. G. Van Silfhout, J. F. Van der Veen, M. S. Finney, A. D. Johnson, and C. Norris, *Phys. Rev. B* **43**, 5001 (1991).

⁶P. J. Orders and B. F. Usher, *Appl. Phys. Lett.* **50**, 980 (1987).

⁷J. M. C. Thornton, A. A. Williams, J. E. McDonald, R. G. Van Silfhout, M. S. Finney, and C. Norris, *Surf. Sci.* **273**, 1 (1992).

⁸S. Tatarenko, J. Cibert, Y. Gobil, G. Feuillet, K. Seminadayar, A. C. Chami, and E. Ligeon, *Appl. Surf. Sci.* **41/42**, 470

(1989).

⁹V. H. Etgens, R. Pinchaux, M. Sauvage-Simkin, J. Massies, N. Jedrecy, N. Greiser, and S. Tatarenko, *Surf. Sci.* **251/252**, 478 (1991).

¹⁰P. Claverie, J. Massies, R. Pinchaux, M. Sauvage-Simkin, J. Frouin, J. Bonnet, and N. Jedrecy, *Rev. Sci. Instrum.* **60**, 2369 (1989).

¹¹M. Sauvage-Simkin, R. Pinchaux, J. Masies, P. Claverie, N. Jedrecy, J. Bonnet, and I. K. Robinson, *Phys. Rev. Lett.* **62**, 563 (1989).

¹²Y. Gobil, J. Cibert, K. Seminadayar, and S. Tatarenko, *Surf. Sci.* **211/212**, 969 (1989).

¹³H. Dosch, B. W. Batterman, and D. C. Wack, *Phys. Rev. Lett.* **56**, 1144 (1986).

¹⁴The correlation length is defined here as $1/\Delta Q$, where $\Delta Q = Q\Delta\theta$, $\Delta\theta$ being the FWHM of the angular scan, mostly controlled by the transverse size of the reciprocal-lattice node since the broadening due to the radial size is integrated over the detector slit width.

¹⁵N. Jedrecy, M. Sauvage-Simkin, R. Pinchaux, J. Massies, N. Greiser, and V. H. Etgens, *J. Cryst. Growth* **102**, 293 (1990).

¹⁶G. Patrat, E. Soyeux, M. Brunel, J. Cibert, S. Tatarenko, and K. Seminadayar, *Solid State Commun.* **74**, 433 (1990).

¹⁷A. Bourret, P. H. Fuoss, A. Rocher, and C. Raisin, in *Symp. Proc. Vol. 208 Advances in Surface and Thin Film Diffraction*, edited by T. C. Wang, P. J. Cohen, and D. J. Eaglesham, MRS Symposia Proceedings No. 208 (Materials Research Society, Pittsburgh, 1991).

¹⁸A. Bourret and P. H. Ruoss (unpublished).

¹⁹A. Bourret, P. H. Fuoss, G. Renaud, and G. Feuillet (private communication).

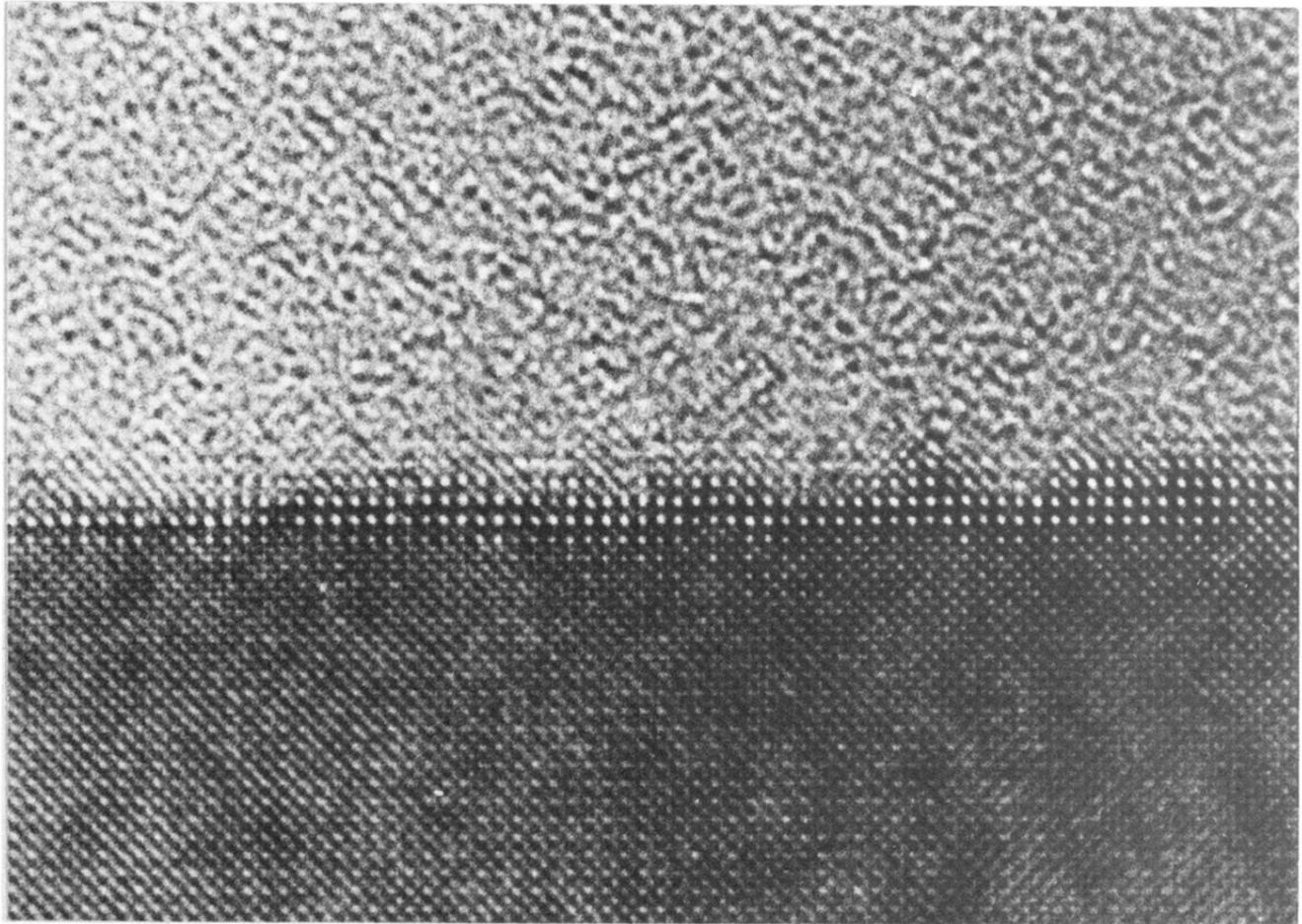


FIG. 3. HRTEM [100] cross section of 2-ML strained ZnTe on GaAs(001) (400 keV).

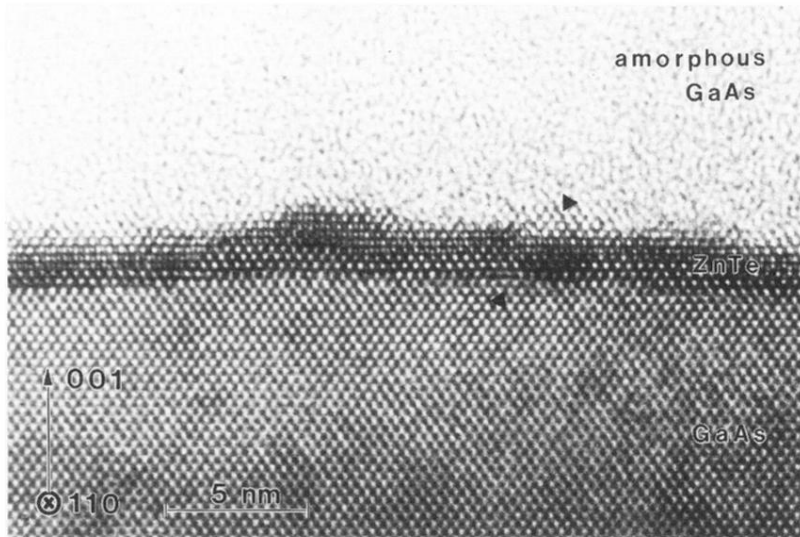


FIG. 4. HRTEM [110] cross section of 5-ML strained ZnTe on GaAs(001) (400 keV), the arrow points to an interface defect in a locally thicker area.

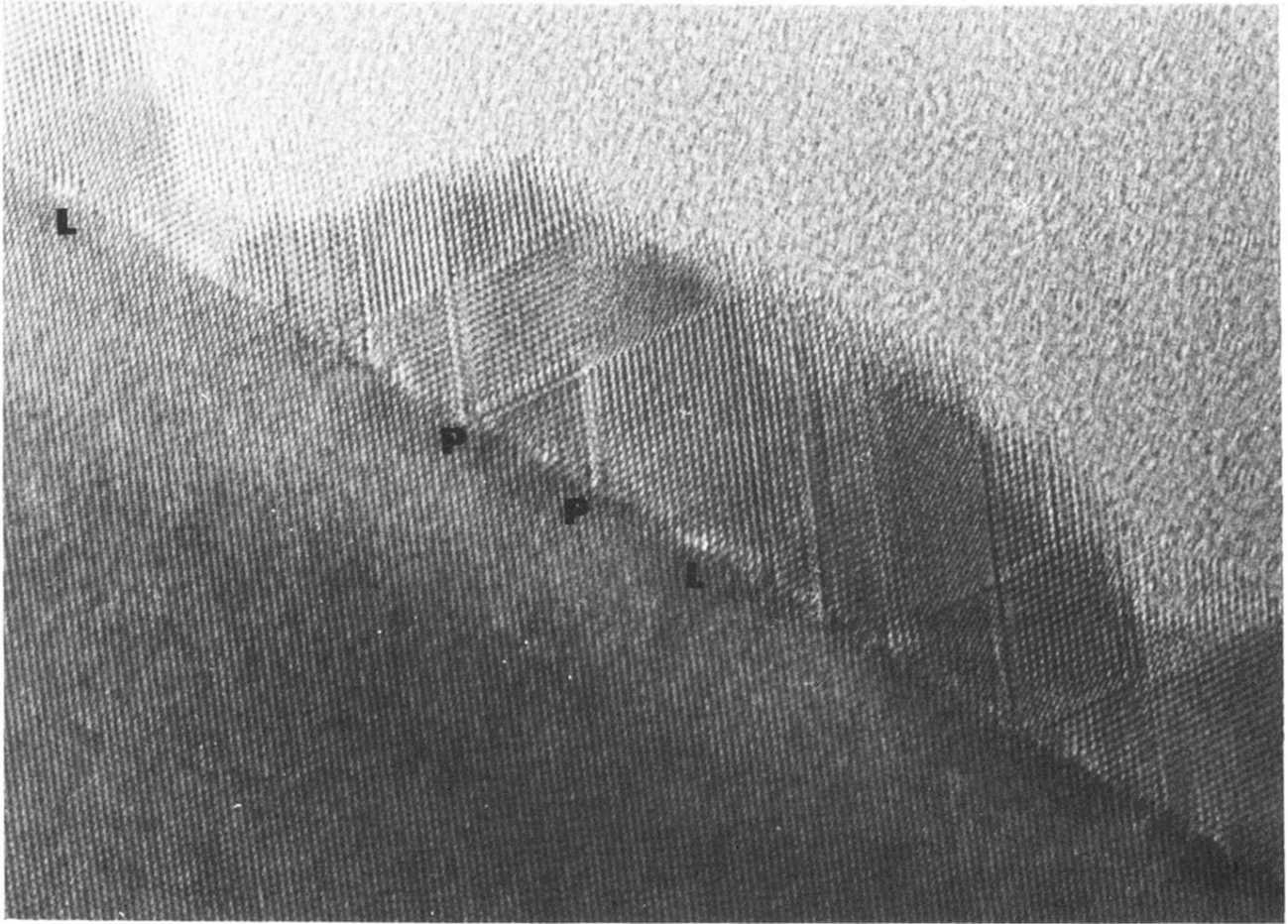


FIG. 5. HRTEM [110] cross section of 35 ML of ZnTe on GaAs(001) (400 keV). Interfaces defects such as Lomer (*L*) and partial (*P*) dislocations are imaged.